ACS APPLIED MATERIALS & INTERFACES

Research Article

www.acsami.org

Electrospun Polystyrene Fiber Diameter Influencing Bacterial Attachment, Proliferation, and Growth

Martina Abrigo,* Peter Kingshott, and Sally L. McArthur

Biointerface Engineering Group, IRIS, Faculty of SET, Swinburne University of Technology, 3122, Hawthorn, Victoria, Australia

ABSTRACT: Electrospun materials have been widely investigated in the past few decades as candidates for tissue engineering applications. However, there is little available data on the mechanisms of interaction of bacteria with electrospun wound dressings of different morphology and surface chemistry. This knowledge could allow the development of effective devices against bacterial infections in chronic wounds. In this paper, the interactions of three bacterial species (*Escherichia coli*, *Pseudomonas aeruginosa*, and *Staphylococcus aureus*) with electrospun polystyrene meshes were investigated. Bacterial response to meshes with different fiber diameters was assessed through a combination of scanning electron microscopy (SEM) and confocal microscopy. Experiments included attachment studies in liquid medium but also directly onto agar plates; the latter was aimed at mimicking a chronic wound environment. Fiber diameter was shown to affect the ability of bacteria to proliferate within the fibrous networks, depending on cell size and shape. The highest proliferation rates occurred when fiber diameter was close to the bacterial size. Nanofibers were found to induce conformational changes of rod shaped bacteria, limiting the colonization process and inducing cell death. The data suggest that simply tuning the morphological properties of electrospun fibers may be one strategy used to control biofilm formation within wound dressings.

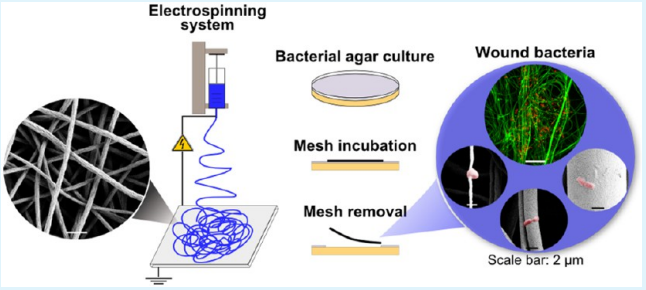

KEYWORDS: *electrospinning, biofilm, fiber diameter, bacteria, chronic wounds, nanofibers*

INTRODUCTION

Nonhealing, or chronic wounds, such as diabetic foot ulcers, pressure ulcers, and venous leg ulcers are complex wounds that do not progress through the usual phases of healing, remaining open or partially healed for several weeks or months.[1,2] These wounds are exposed to a high risk of bacterial infection as they become contaminated by a complex population of many different bacteria, that find the right conditions (i.e., moisture, pH, and temperature) to proliferate and develop into biofilm.[3]

Polymeric micro/nanofibrous meshes are promising candidates for chronic wound care because they have been shown to promote hemostasis, fluid absorption, cell respiration, and gas permeation.[4] Meshes are formed from fibers with diameters ranging from several micrometers down to few nanometers.[5] Among the range of techniques available to fabricate meshes, electrospinning is most frequently chosen because it is a simple, cost-effective, and versatile process. Electrospinning is based on the application of a high voltage to the selected polymer solution or melt to induce the formation of a micro/nanometric filament which is drawn toward a collector. After a certain time, a fibrous structure made of polymeric nonwoven or aligned fibers can be collected.[6] Over the past ten years, electrospun materials have been widely investigated for tissue engineering applications. Fiber diameter, interfiber distance, and fiber alignment have all been found to significantly affect the ability of cells to adhere onto the electrospun scaffolds and proliferate within the fibrous network to form tissue.[7,8] Researchers have also developed different strategies to create electrospun meshes with the ability to encourage the wound healing processes, including the encapsulation of vitamins, growth factors, and natural compounds into or onto the fibers.[2]

To our knowledge, despite bacterial infection representing a major challenge in chronic wound care, studies on the mechanisms of adhesion, spreading, and colonization of electrospun meshes by bacteria do not exist. Antibiotics and antimicrobials have been loaded into the fibers to be released in the wound in an attempt to address wound infection,[2] but few studies have examined the interactions between fibers and individual bacteria. Bacterial attachment on flat substrates and the factors that influence this process have been widely investigated as researchers attempt to design antibacterial or antifouling surfaces.[9] Theoretical approaches, thermodynamic theories, and cell studies have provided important insights on the mechanisms that control bacterial adhesion and on the role played by cell surface properties.[9,10] It is currently recognized that, apart from cell surface characteristics, bacterial attachment mechanisms are also regulated and influenced by a wide range of substratum properties, such as morphology, surface chemistry, and roughness.[9] The mechanisms that bacteria use to adhere to flat surfaces with different chemistries and

Received: January 15, 2015
Accepted: March 23, 2015
Published: March 23, 2015

DOI: 10.1021/acsami.5b00453
ACS Appl. Mater. Interfaces 2015, 7, 7644−7652

nanotopographies have been reviewed in detail by Mitik-Dineva et al.[10] The work that most closely approaches the question on the interactions of bacteria with fibrous substrates was provided by Kargar et al.[11] They investigated the state of adhesion of *P. aeruginosa* bacteria to polystyrene (PS) flat surfaces texturized with aligned PS fibers with different diameters and spacing. The adhesion mode of *P. aeruginosa* on texturized surfaces was found to be dependent on fiber diameter and spacing, suggesting that strategically designed curvatures can reduce the bacterial adhesion process.[11]

In the present work, the response of bacteria to electrospun micro/nanofibrous meshes with different average fiber diameters was investigated. Meshes were fabricated in PS through the electrospinning process in three average fiber diameter ranges. PS was chosen as a model system being the standard material used to fabricate tissue culture plates for *in vitro* cell and bacterial culture; moreover, PS is a nondegradable synthetic polymer which allowed us to study the role of fiber morphology preventing additional uncertainties, such as polymer degradation that occurs in the presence of materials most frequently chosen for wound healing meshes, such as poly(lactic acid), poly(glycolic acid), and copolymers.[12] To find the best approach to mimic the wound environment, two methods of bacterial culturing (solution and agar cultures) were performed. *E. coli* bacteria were used for the solution culture as this is a most simplistic model of the wound environment. The other two bacterial species (*P. aeruginosa* and *S. aureus*) most frequently involved in chronic wound infection[3,16] were included in the agar experiment design as this constitutes a more realistic model that better mimics a wound bed. The attachment and growth of bacteria in and on the meshes was assessed using a combination of scanning electron microscopy (SEM) and confocal microscopy after cell viability staining. The performed biological assays are standard protocols traditionally used to assess bacterial species (Gram staining) and viability (LIVE/DEAD assay). These assays were adapted to investigate the adhesion and spreading of bacteria within fibrous meshes in the attempt of overcoming one of the main challenges associated with characterizing biological phenomena occurring at the interface with three-dimensional nanostructured systems.

MATERIALS AND METHODS

Materials. For the electrospinning of the micro/nanofibrous meshes, PS (MW = 250,000) was purchased from Acros Organics; ethanol and dimethylformamide (DMF) were both supplied from Science Supply Australia Pty Ltd. (AR grade, 100% purity). The surfactant sodium dodecyl sulfate (SDS) was obtained from Chem-Supply (Australia). 1.5% w/v tryptic soy agar (TSA) and tryptic soy broth (TSB) for bacterial cultures were purchased from ThermoFisher Scientific (Australia). LIVE/DEAD assay was performed using the LIVE/DEAD BacLight, Bacterial Viability Kits (3.34 mM propidium iodide (PI) in dimethyl sulfoxide (DMSO) and 20 mM of SYTO 9 in DMSO) purchased from Invitrogen Life Technologies (Australia). Crystal violet 1% aqueous solution was purchased from Sigma-Aldrich (Australia). *E. coli*, *P. aeruginosa*, and *S. aureus* strains used in this study were clinical isolates purchased from American Type Culture Collection (25922 ATCC).

Electrospinning. A home-built apparatus in horizontal configuration was used to fabricate the PS meshes. PS was dissolved overnight in DMF. Four solutions at polymer concentrations of 10% w/v, 15% w/v, 20% w/v with 0.1% w/v SDS, and 30% w/v were electrospun. Electrospinning parameters (applied voltage, flow rate, and needle collector distance) were selected for each concentration to ensure uniform and continuous spinnability. The values of the electrospinning parameters that were selected for each solution are shown in Table 1. The blunt needle diameter was selected depending on the polymer concentration: 22 gauge for 15%, 18 gauge for 30%, and 24 gauge for 10% and 20% PS with surfactant. A grounded metal plate 20 × 20 cm^2 coated with aluminum foil was used as collector for the deposition of the meshes. To fabricate meshes with suitable thickness (~1 mm) to enable handling during the bacterial assays, the electrospinning of the 10% and 20% with surfactant solutions was performed for 4 h, 2 h, and 30 min for the 15% solution and 1 h for the 30% solution. The side of the mesh which was adhering onto the aluminum foil will be referred as the back of the mesh. After electrospinning, the foil was cut into 2 × 2 cm^2 squares which were immersed into ethanol aqueous solution (70% v/v) for 30 s, with the mesh facing down. The aluminum foil was gently removed from the back of each mesh using tweezers. Meshes were then transferred into 6-well plates, facing up. The conductivity of the polymer solutions was measured using the SevenCompact S230 conductivity meter from Mettler Toledo (Australia).

Table 1. Process Parameters Selected for the Electrospinning of PS Solutions at Different Concentrations

polymer [% w/v]	surfactant [% w/v]	V^a [kV]	flow rate [μL/h]	N−C^b [cm]
10		15	600	15
15		18	800	20
20	0.1	14	500	15
30		16	1000	18

^{a}Applied voltage. ^{b}Needle−collector distance.

X-ray photoelectron spectroscopy (XPS) analysis of the meshes was performed using a Kratos AXIS NOVA spectrometer (Kratos Analytical Inc., Manchester, UK) using a monochromated Al Kα X-ray source at a power of 150 W. All elements present were identified from survey spectra (acquired at a pass energy of 160 eV). The atomic concentrations of the detected elements were calculated using integral peak intensities and the sensitivity factors supplied by the manufacturer.

Bacterial Culture. Electrospun meshes were sterilized in ethanol aqueous solution (70% v/v) for 30 min and rinsed 3 times with Milli-Q water. A 1.5% TSA plate was inoculated with *E. coli* thawed from a −80 °C stock. The plate was incubated for 18 h at 37 °C. A single bacterial colony was transferred from the agar plate into 30 mL of TSB in a 50 mL tube. The culture was incubated for 18 h (37 °C, 120 rpm) and consequently centrifuged for 15 min (25 °C, 2480 relative centrifugal force (rcf)). The obtained pellet was resuspended in 30 mL of clean TSB and diluted up to an optical density ($O.D._{600nm}$) of 0.3. For the solution experiment, 3 mL of the inoculated TSB was transferred on the electrospun meshes and incubated (37 °C, 120 rpm) for 1 h. For the agar experiments, 100 μL of the broth culture was transferred onto an agar plate and spread onto the surface of the plate through a sterile spreader. The plate was incubated for 18 h at 37 °C. After incubation, a confluent biofilm of *E. coli* cells was obtained. As the fibers were spun onto a collector surface, the resulting mesh had an orientation, with the fibers that were in immediate contact with the collector being slightly deformed due to the contact. As such, in the study, the meshes were placed on the agar with the front of the mesh facing down onto the biofilm and the collector-surface facing up. Meshes were incubated for 1 h at 37 °C. After incubation, the culture was observed for the presence of an inhibitory ring around the meshes. A silver impregnated mesh was used as control. The same procedure was repeated for *P. aeruginosa* and *S. aureus*.

SEM. The morphological properties of PS fibers electrospun with different process parameters were analyzed and compared through SEM (ZEISS Supra 40 VP Carl Zeiss SMT, Germany, EHT = 3 kV) images. Prior the SEM analysis, fibers were gold coated (10−15 nm) using the Dynavac CS300 thermal deposition chamber. To measure the average fiber diameter for each set of electrospinning parameters, three meshes were electrospun; on each mesh, 3 SEM images at the same magnification were taken. On each image, 10 fibers were

DOI: 10.1021/acsami.5b00453
ACS Appl. Mater. Interfaces 2015, 7, 7644−7652

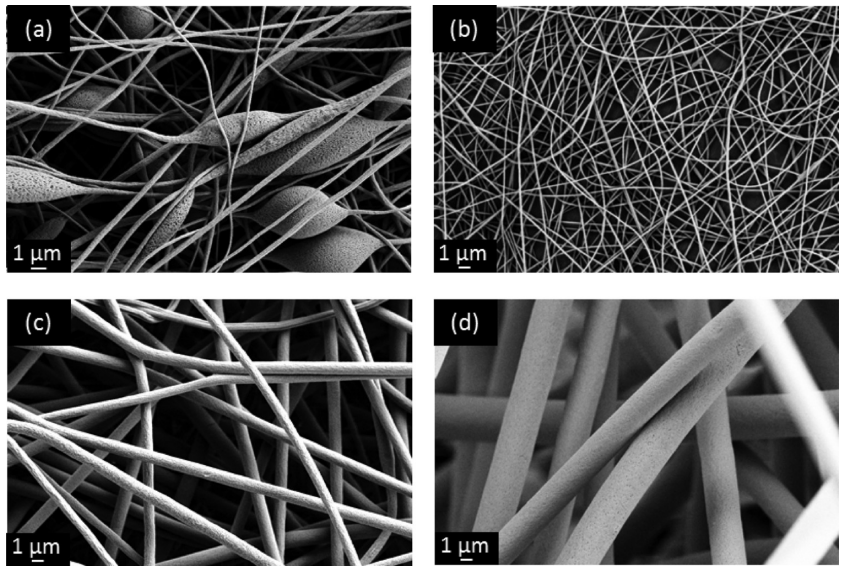

Figure 1. SEM images of PS meshes electrospun from solutions in DMF at four concentrations: (a) C = 10% w/v, Φ = 300 ± 200 nm; (b) C = 20% w/v with surfactant, Φ = 500 ± 200 nm; (c) C = 15% w/v, Φ = 1000 ± 100 nm; (d) C = 30% w/v, Φ = 3000 ± 1000 nm.

randomly selected and the diameter was measured through ImageJ software. Therefore, the average fiber diameter of the meshes was calculated by averaging 90 values in total for each set of parameters tested.

SEM images were also used to explore initial bacterial adhesion and progressive spreading and colonization of PS electrospun meshes exposed to *E. coli*, *P. aeruginosa*, and *S. aureus* cultures. For both solution and agar experiments, after incubation, the meshes were rinsed 3 times with Milli-Q water, to remove the bacteria which were not adhered onto the fibers. Two mL of formaldehyde solution in phosphate buffered saline (PBS) (3.4% v/v) was added to the samples for 10 min for bacterial fixation. Samples were rinsed once with Milli-Q water and exposed to 3 subsequent rinses in ethanol aqueous solutions at increasing concentrations for dehydration; samples were finally left in pure ethanol for 5 min. When dry, meshes were mounted on SEM support and gold coated. Experiments were performed in triplicates.

LIVE/DEAD Assay. To investigate the influence of fiber diameter on bacterial behavior, the LIVE/DEAD assay was performed. LIVE/DEAD is a two color fluorescence assay of bacterial viability. After staining, when excited at 480−490 nm, bacteria emit green fluorescence (emission wavelength 500 nm) if alive and red fluorescence (emission wavelength 635 nm) if dead. For both solution and agar experiments, after incubation, meshes were rinsed 3 times with PBS, to remove the bacteria which were not adhered. LIVE/DEAD staining solution was prepared according the company's instructions. Two mL of the LIVE/DEAD solution was added to each sample for 30 min. Meshes were incubated at 37 °C in the dark. The staining solution was removed, and samples were rinsed once with PBS. Samples were imaged under an OLYMPUS FV1000D Laser Confocal Scanning Microscope with OLYMPUS 40× and 100× objectives. Selected filters were U-MNIBA filter (excitation 470−490 nm, green emission) and U-MWIG2 filter (excitation 510−550 nm, red emission). Olympus FluoViewer software was used for image capturing and processing. The experiment was performed in triplicates.

Crystal Violet Assay. After a 1 h incubation on the *E. coli*, *P. aeruginosa*, and *S. aureus* agar cultures, meshes were removed from the plates. Five mL of 1:100 dilution of crystal violet aqueous solution in NaCl 0.85% w/v was added to each plate and incubated for 10 min in the dark. The dilution was then removed, and plates were rinsed three times with NaCl 0.85% w/v. Photographs of the stained plates were taken.

RESULTS AND DISCUSSION

Characterization of Electrospun Meshes. Solutions of PS dissolved in DMF were electrospun to fabricate meshes with controlled morphology and average fiber diameter (Φ). Polymer concentration was a significant parameter affecting Φ. Figure 1 shows the SEM micrographs of the meshes electrospun from PS solutions at different concentrations. 10% w/v resulted in the formation of nanofibers (Φ_0 = 300 ± 200 nm), but occasional defects in the form of beads and polymer agglomerates were also present within the mesh (Figure 1a). The increase of polymer concentration to 20% w/v combined with the addition of 0.1% w/v SDS also allowed the fabrication of fibers in the nanoscale (Φ_1 = 500 ± 200 nm) but prevented the formation of defects (Figure 1b). A solution of 15% w/v resulted in the increase of average fiber diameter to Φ_2 = 1000 ± 100 nm and in the formation of uniform fibers with no defects (Figure 1c). When the polymer concentration was increased to 30% w/v, average fiber diameter further increased to Φ_3 = 3000 ± 1000 nm (Figure 1d). Table 2 summarizes the average fiber diameters obtained for each polymer concentration and shows the measured values of solution conductivity. The addition of the 0.1% w/v surfactant to 20% w/v PS solution resulted in a significant increase of solution conductivity to 57 μS/cm in comparison to the other solutions (0.3−1.5 μS/cm). The increase in solution conductivity allowed the fabrication of nanofibers preventing the formation of defects. For the following experiments, the three sets of meshes with average fiber diameters Φ_1, Φ_2, and Φ_3 were used.

Table 2. Properties of PS Solutions for the Electrospinning of Meshes with Controlled Average Diameter

sample	polymer [% w/v]	surfactant [% w/v]	Φ^a [nm]	conductivity [μS/cm]
Φ_0	10		300 ± 200	1.5
Φ_1	20	0.1	500 ± 200	57
Φ_2	15		1000 ± 100	0.5
Φ_3	30		3000 ± 1000	0.3

[a]Average fiber diameter.

DOI: 10.1021/acsami.5b00453
ACS Appl. Mater. Interfaces 2015, 7, 7644−7652

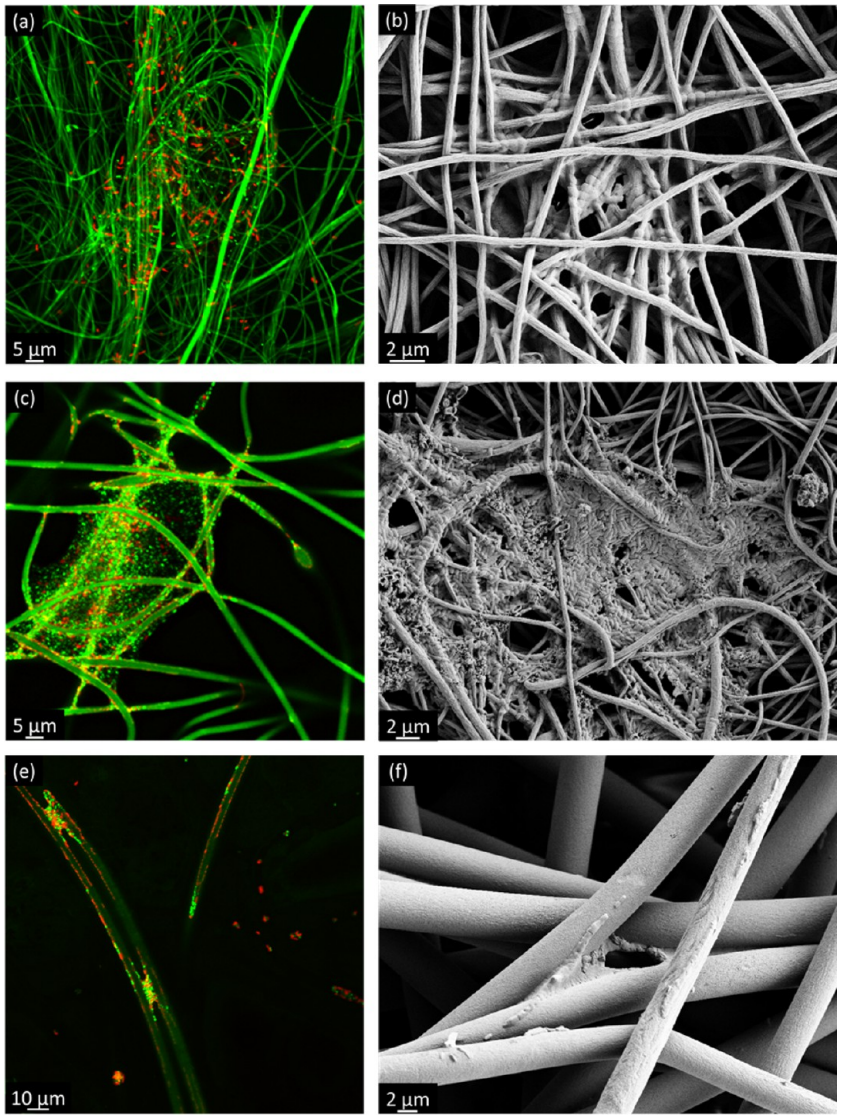

Figure 2. Bacterial solution culture experiment. Confocal (a, c, e) and SEM (b, d, f) images of *E. coli* cells colonizing PS electrospun meshes with fiber diameter ranges of: (a, b) Φ_1 = 500 ± 200 nm; (c, d) Φ_2 = 1000 ± 100 nm; (e, f) Φ_3 = 3000 ± 1000 nm.

The mesh Φ_0 was excluded due to the presence of defects. To analyze the surface chemistry of the selected sets of meshes, XPS was performed. The elemental analysis of all the meshes showed their surface composition to be 99−100% carbon with trace amounts of oxygen and nitrogen. The presence of these elements on the surface of the fibers is due to the exposure of the fibers to impurities that is intrinsically involved in the electrospinning process. Critically, there was no sulfur detected on the surface of the Φ_1 meshes, indicating that the addition of 0.1% SDS to the polymer solution did not affect the surface chemistry of the resultant fibers.

Influence of Fiber Diameter on Bacterial Behavior. *E. coli Attachment in Solution.* To confirm the XPS results and ensure that the Φ_1 mesh did not leach residual surfactant when exposed to a culture of bacteria, an inhibitory zone experiment was performed. While the control sample (silver impregnated mesh) produced a clear zone of inhibition, killing the cells it came in contact with on the agar, no ring was detected around the Φ_1 mesh.

To investigate the influence of fiber diameter on bacterial behavior, the Φ_1, Φ_2, and Φ_3 meshes were exposed to a solution culture of *E. coli*. SEM images were used to monitor the spreading of bacteria within the mesh; confocal images were taken after performing the LIVE/DEAD assay to visualize the distribution of live and dead cells within the samples. The influence of fiber diameter on the ability of *E. coli* cells to spread within the mesh and form colonies is shown in Figure 2. In the confocal images (Figure 2a,c,e), fibers are fluorescing green due to the autofluorescence of the PS material. Bright green and red spots corresponding to live and dead bacterial cells, respectively, can be clearly visualized. A distinctive manner of colonizing the mesh depending on the average fiber diameter was found to occur. When $\Phi = \Phi_1$ (Figure 2a), a high prevalence of dead bacterial cells was present within the mesh. Bacteria appeared to be mainly isolated cells adhering onto the surface of the fibers. This was confirmed by SEM images (Figure 2b), where cells were found to adhere onto and wrap around the surface of the fibers. Few cells appeared to bridge from the surface of the fibers toward the interstices. Clusters of bacteria formed within the mesh, but due to the small size of the fibers, bacteria appeared to find it difficult to create compact colonies on the fibrous network. When the fiber diameter was

DOI: 10.1021/acsami.5b00453
ACS Appl. Mater. Interfaces 2015, 7, 7644−7652

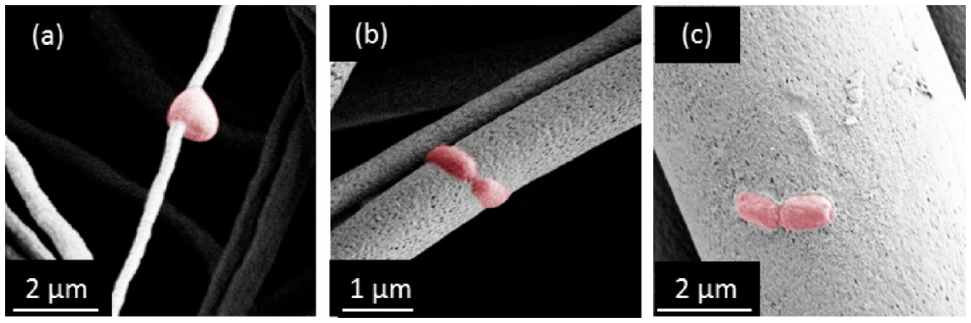

Figure 3. SEM of single *E. coli* cells (falsely colored in red) adhered onto PS electrospun fibers with diameter of: (a) 0.3 μm (b); 1 μm; (c) 5 μm.

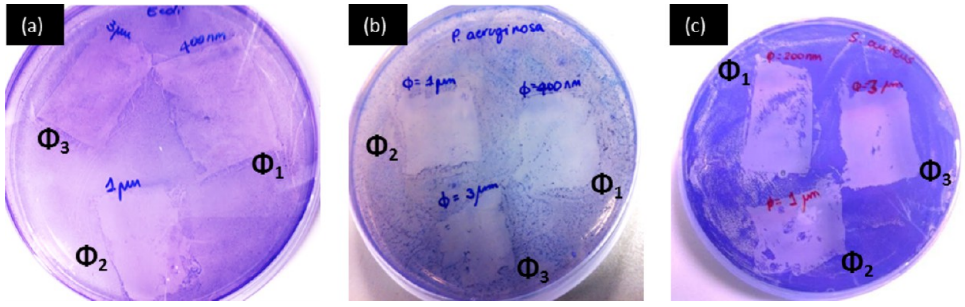

Figure 4. Bacterial agar culture experiment. Crystal violet staining of agar cultures after mesh removal: (a) *E. coli*; (b) *P. aeruginosa*; and (c) *S. aureus*.

in the range of Φ_2, bacteria appeared to be able to bridge across fibers and create colonies that used the fibrous substrate as a scaffold, supporting and encouraging cell growth and spreading. Figure 2c shows a colony of *E. coli* cells adhered over tens of fibers. A high proportion of live cells can be seen on the surface of the fibers as well as throughout the colony in the interstices. The SEM image (Figure 2d) confirmed the presence of a compact colony spread throughout the mesh. The darker agglomerates on the surface of the mesh correspond to the extracellular polymeric substance (EPS) that bacteria themselves produce to ensure adhesion onto a surface and to each other. When the fiber diameter was greater than the bacterial size ($\Phi = \Phi_3$), *E. coli* cells appeared to consider each fiber surface as a flat substrate. Most of the bacteria were aligned along single fibers in the form of a train (Figure 2e,f). In response to crossing over points among two or more fibers, bacteria were able to proliferate across the fibers, producing agglomerates of cells.

The response of isolated *E. coli* cells to single fibers in the three diameter ranges is shown in Figure 3, where the cells are falsely colored in red. When $\Phi = \Phi_1$ (Figure 3a), the cell appeared to wrap around the fiber to achieve complete adhesion, thus assuming a round shape. When $\Phi = \Phi_2$ (Figure 3b) or bigger (Figure 3c), the cells could easily adhere onto the surface maintaining their original rod-like shape. This behavior suggests that prevalence of dead isolated cells found on the Φ_1 meshes could be due to the fact that the distortion of *E. coli* cells, required to adhere onto the surface of the fibers, affects bacterial function and viability. The change of bacterial shape induced by the small size of the fibers could impair the ability of bacteria to bridge across fibers and produce EPS for developing colonies.

Agar-Mesh Cell Transfer. Colonized or infected wounds are solid substrates contaminated by a variety of bacterial species. In an attempt to at least in part mimic this environment, confluent biofilms of bacteria were grown on agar plates. The agar experiment design constitutes a more realistic model that better mimics a wound bed compared to the bacterial culture in solution. Since chronic wounds are contaminated by a variety of bacteria, three bacterial species most frequently responsible for wound infection were chosen: *E. coli*, *P. aeruginosa*, and *S. aureus*. The capacity of the meshes to attract and remove the bacterial cells from the agar plates was tested by staining the agar plate with crystal violet (CV) after mesh removal. Figure 4 shows (a) *E. coli*, (b) *P. aeruginosa*, and (c) *S. aureus* agar cultures where the mesh was in contact for 1 h and then removed. The images clearly show that the meshes attracted and removed most of the bacteria cells present on the three agar cultures.

The meshes were also analyzed after removal from the agar plates for the presence of bacteria, using SEM and confocal microscopy. Figure 5a shows LIVE/DEAD stained *E. coli* cells colonizing the Φ_1 mesh. The image shows a high prevalence of dead cells and a few clusters of live bacteria. In the SEM image (Figure 5b), single bacterial cells can be seen to have adhered onto and wrapped around the surface of the fibers; cell clusters correspond with fiber crossover or adjacent fibers. When the fiber diameter was in the range of Φ_2, bacterial cells proliferated within the fibrous network, using the fibers as a support to move across the interstices of the mesh. The confocal image (Figure 5c) reveals a high prevalence of live bacteria, both adhered onto the surface of the fibers and clustered within the colony. The SEM micrograph (Figure 5d) shows that bacteria have been capable of progressively colonizing a region of the mesh composed of tens of fibers, developing a compact system in which each cell is supporting the adjacent ones. On the larger diameter fibers (Φ_3), bacteria tended to adhere onto the fiber surface and preferentially proliferate along single fibers, creating trains of aligned cells. Aligned bacterial colonies are also found between two adjacent fibers; agglomerates of cells can be seen between two or more fibers in areas of fiber cross over (Figure

DOI: 10.1021/acsami.5b00453
ACS Appl. Mater. Interfaces 2015, 7, 7644−7652

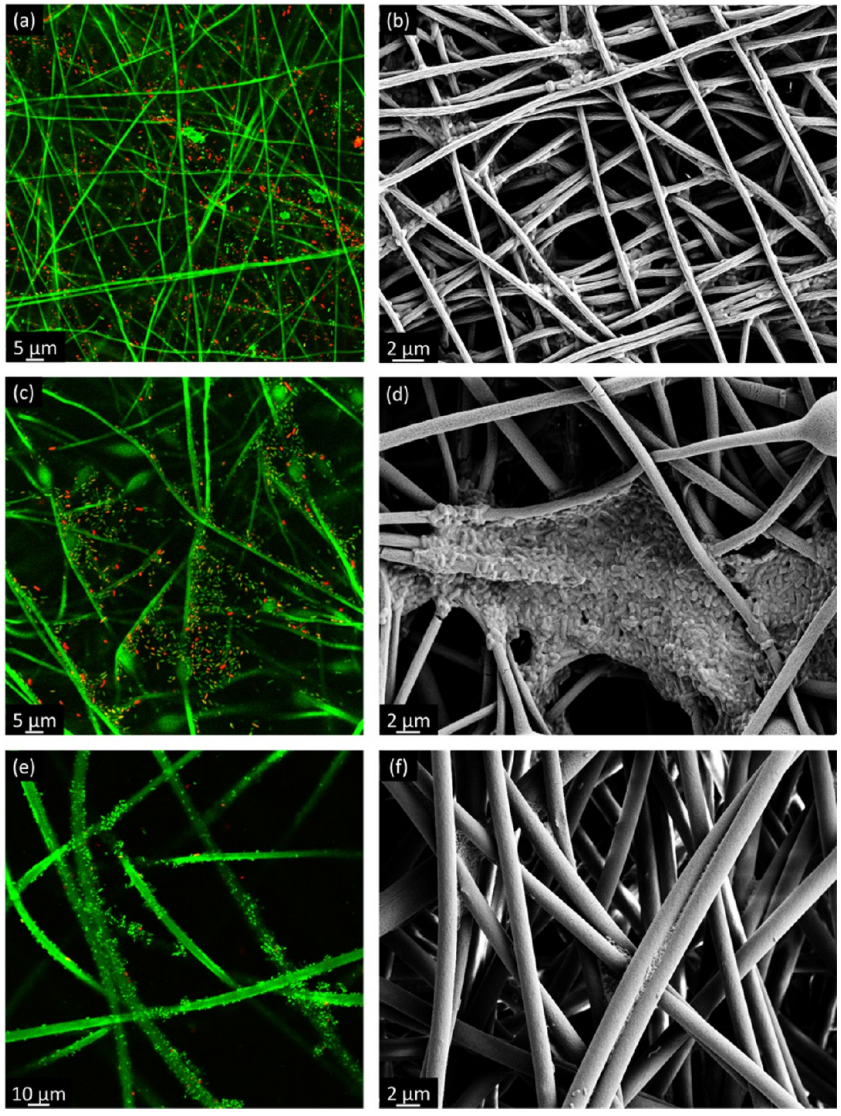

Figure 5. Bacterial agar culture experiment. Confocal (a, c, e) and SEM (b, d, f) images of *E. coli* cells colonizing PS electrospun meshes with fiber diameter ranges of: (a, b) Φ_1 = 500 ± 200 nm; (c, d) Φ_2 = 1000 ± 100 nm; (e, f) Φ_3 = 3000 ± 1000 nm.

5f). The confocal image (Figure 5e) shows a high prevalence of live bacteria proliferating along the fibers.

Results showed that the Φ_2 meshes, when exposed to *E. coli* solution or agar cultures, acted as a scaffold, supporting and encouraging cell proliferation along the fibers and through the interstices. The *P. aeruginosa* response to different fiber sizes (Figure 6) was similar to *E. coli*, where cells colonizing the Φ_1 meshes were prevalently dead and isolated onto the fibers (Figure 6a). The SEM magnification of the mesh (Figure 6b) shows single cells adhered and wrapped around the fibers as well as small agglomerates of cells at the crossing over points between fibers. The Φ_2 mesh provided the best support for bacteria to adhere, spread, and proliferate. Figure 6c shows a high prevalence of live cells not only colonizing the fiber surface but also spread throughout the fibrous network; Figure 6d shows that after a 1 h incubation the cells that were attached onto the fiber surface were in the process of creating bridges among the fibers and creating a progressively spread out colony. Cells visibly appeared embedded in EPS that ensures the support of the colony and the adhesion between adjacent cells. Cells were glued together in the empty spaces among the fibers throughout the mesh where there is no other support than the EPS to sustain them. As previously found for *E. coli*, when $\Phi = \Phi_3$, *P. aeruginosa* preferentially proliferated along the fiber surface. A high prevalence of live cells is present in the confocal images (Figure 6e), indicating that bacterial adhesion and proliferation were not impaired; SEM images showed that bacteria tended to proliferate randomly on the fiber surface, without following the alignment trend that was found recurrent for *E. coli*. Small cell agglomerates can be seen between fibers crossing over each other, although most cells covered the fiber surface (Figure 6f).

S. aureus cells were found to proliferate and cover the entire Φ_1 mesh after 1 h of incubation. Figure 7a shows colonies of live bacteria throughout the fibrous network, with a very low percentage of dead cells. The SEM micrograph (Figure 7b) confirms that *S. aureus* cells adhered onto the fiber surface and proliferated within the mesh forming a compact system of cells, supporting each other. When the larger fibers (Φ_2 and Φ_3) were exposed to the bacterial culture, cells adhered and proliferated predominantly along the fiber surface. Figure 7c,e shows a high prevalence of live bacteria attached onto the Φ_2

DOI: 10.1021/acsami.5b00453
ACS Appl. Mater. Interfaces 2015, 7, 7644−7652

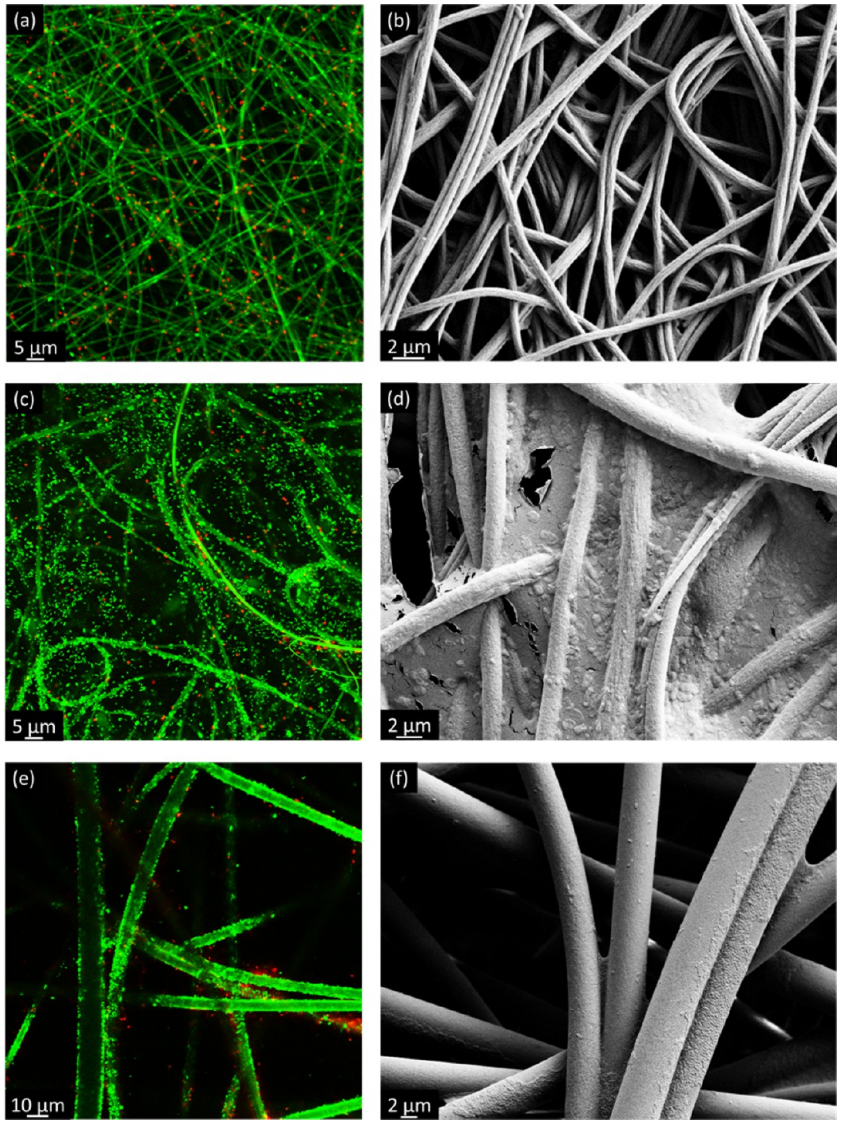

Figure 6. Bacterial agar culture experiment. Confocal (a, c, e) and SEM (b, d, f) images of *P. aeruginosa* cells colonizing PS electrospun meshes with fiber diameter ranges of: (a, b) Φ_1 = 500 ± 200 nm; (c, d) Φ_2 = 1000 ± 100 nm; (e, f) Φ_3 = 3000 ± 1000 nm.

and Φ_3 fibers, respectively. The tendency of bacteria to attach and proliferate onto the fibers is evident from Figure 7d,f, where little evidence of bridging among fibers and colonizing the interstices of the meshes can be seen.

E. coli and *P. aeruginosa* are Gram-negative rod shaped bacteria 1−2 μm long, that were found to have similar responses when interacting with all three sets of meshes. The Φ_2 mesh was composed of fibers with diameter close to the cell length. In this case, the mesh was found to act as a scaffold, encouraging bacterial growth throughout the fibrous substrate. Bacteria formed compact colonies in the interstices among fibers through the production of EPS that ensures the support of the cells. On the Φ_1 mesh, where fiber size was smaller than the bacterial length, a distortion of the cell shape occurred, resulting in a high prevalence of dead cells. Fiber diameters larger than the bacterial length (Φ_3) resulted in cells predominantly proliferating onto the surface of the fibers following aligned or random directions, with a low degree of bridging among and across fibers.

S. aureus, a Gram-positive round shape bacterium 0.5−1 μm in diameter, showed the highest proliferation rate with the Φ_1 mesh, where fiber diameter was close to bacterial size. On the Φ_2 and Φ_3 meshes, where fiber diameter was bigger than the bacterial size, *S. aureus* preferentially proliferated onto the surface of the fibers.

These results show that the average fiber diameter of the mesh does influence the capacity of bacteria to adhere, proliferate, and form colonies. This influence is directly linked to bacterial size and shape. In fact, results show that, for the three bacterial species considered, the highest spreading and proliferation was found to occur when the fiber diameter was close to bacterial size. These findings can be related to the "attachment points" theory, according to which organisms smaller than the scale of the surface texture have greater adhesion strength due to the availability of multiple attachment points, in comparison to microorganisms that are larger than the surface texture.[13,14] The theory also states that small round shape bacteria, such as *S. aureus*, exhibit a different attachment pattern compared to the bigger, elongated cells, due to the different number of accessible attachment points. This is in agreement with the fact that *S. aureus* was found to have the highest attachment and proliferation rate on the smallest Φ_1

DOI: 10.1021/acsami.5b00453
ACS Appl. Mater. Interfaces 2015, 7, 7644−7652

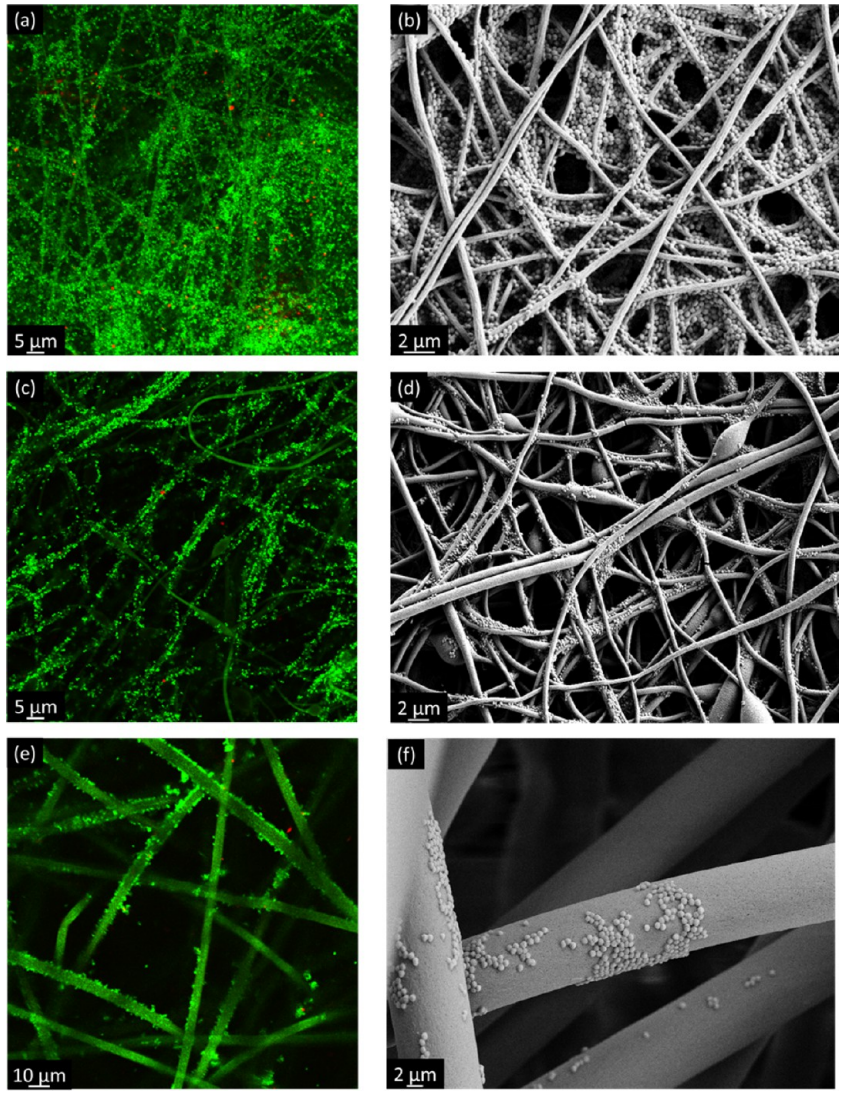

Figure 7. Bacterial agar culture experiment. Confocal (a, c, e) and SEM (b, d, f) images of *S. aureus* cells colonizing PS electrospun meshes with fiber diameter ranges of: (a, b) Φ_1 = 500 ± 200 nm; (c, d) Φ_2 = 1000 ± 100 nm; (e, f) Φ_3 = 3000 ± 1000 nm.

fibers, while the rod shape bacteria colonized the Φ_2 mesh preferentially.[15] These findings open up the possibility to design fibrous meshes of heterogeneous morphology to suppress the growth of different bacterial species in a complex environment such as a chronic wound bed.

CONCLUSION

The diameter of electrospun PS fibers was shown to influence the ability of three bacterial species to proliferate and colonize the fibrous substrate. SEM and confocal images indicated that bacterial spreading throughout the mesh depended on fiber diameter and bacterial size and shape. Meshes with an average fiber diameter close to bacterial size were found to offer the best support for bacterial adhesion and spreading, constituting a scaffold that bacteria use as a framework for forming colonies. For rod shape elongated cells (*E. coli* and *P. aeruginosa*), fiber diameters smaller than the bacterial length resulted in most cells wrapping around each fiber, thus limiting the ability of bacteria to easily create bridges across fibers and form colonies. These bacteria exhibited similar behavior, colonizing preferentially the 1 μm meshes. Round *S. aureus* cells showed the highest proliferation throughout the nanofibrous substrates; in the presence of bigger fibers, *S. aureus* cells preferentially adhered on the fiber surface, without spreading throughout the mesh.

The presented results show the possibility of using fiber size as a tool to control bacterial adhesion and spreading into electrospun materials. In the attempt of designing wound dressings capable of controlling the bacterial load in the wound bed, the control over fiber size could be one of the strategies to reduce the risk of wound infection. These results also underline the complexity of the environment that wound dressings are designed to interact with. Bacteria with different morphologies were shown to respond in a distinctive manner to different fiber sizes; since chronic wounds are contaminated by a variety of bacteria, with different sizes and shapes, fiber diameter may not be the only strategy used to limit the bacterial load in the wound bed. The control over fiber size could potentially be combined with strategically designed additional fiber properties, such as surface chemistry or controlled release. Apart from providing a device that could minimize bacterial growth in a wound bed, the possibility also exists for developing a mesh capable of attracting bacteria from the wound bed; the mesh

DOI: 10.1021/acsami.5b00453
ACS Appl. Mater. Interfaces 2015, 7, 7644−7652

with controlled fiber diameter could constitute a trap to be used to clean up the wound.

AUTHOR INFORMATION

Corresponding Author

*E-mail: mabrigo@swin.edu.au.

Notes

The authors declare no competing financial interest.

ACKNOWLEDGMENTS

This work was supported by L. E. W. Carty Foundation. Authors thank Dr. T. Ameringer for technical assistance with the electrospinning. M.A. also acknowledges Swinburne Chancellor's Research Scholarship (CRS). This work was performed in part at the Biointerface Engineering Hub @ Swinburne part of the Victorian Node of the Australian National Fabrication Facility, a company established under the National Collaborative Research Infrastructure Strategy to provide nano- and microfabrication facilities for Australia's researchers.

REFERENCES

(1) Enoch, S.; Leaper, D. J. Basic Science of Wound Healing. *Surgery (Oxford)* **2005**, *23*, 37−42.

(2) Abrigo, M.; McArthur, S. L.; Kingshott, P. Electrospun Nanofibers as Dressings for Chronic Wound Care: Advances, Challenges, and Future Prospects. *Macromol. Biosci.* **2014**, *14*, 772−792.

(3) Garth, J. A.; Swogger, E.; Wolcott, R.; Pulcini, E.; Secor, P.; Sestrich, J.; Costerton, J. W.; Stewart, P. S. Biofilms in Chronic Wounds. *Wound Repair Regener.* **2008**, *16*, 37−44.

(4) Zhang, Y.; Lim, C.; Ramakrishna, S.; Huang, Z.-M. Recent Development of Polymer Nanofibers for Biomedical and Biotechnological Applications. *J. Mater. Sci.: Mater. Med.* **2005**, *16*, 933−946.

(5) Zahedi, P.; Rezaeian, I.; Ranaei-Siadat, S.-O.; Jafari, S.-H.; Supaphol, P. A Review on Wound Dressings with an Emphasis on Electrospun Nanofibrous Polymeric Bandages. *Polym. Adv. Technol.* **2010**, *21*, 77−95.

(6) Burger, C.; Hsiao, B. S.; Chu, B. Nanofibrous Materials and Their Applications. *Annu. Rev. Mater. Res.* **2006**, *36*, 333−368.

(7) Sun, T.; Norton, D.; McKean, R. J.; Haycock, J. W.; Ryan, A. J.; MacNeil, S. Development of a 3D Cell Culture System for Investigating Cell Interactions with Electrospun Fibers. *Biotechnol. Bioeng.* **2007**, *97*, 1318−1328.

(8) Nisbet, D. R.; Forsythe, J. S.; Shen, W.; Finkelstein, D. I.; Horne, M. K. Review Paper: A Review of the Cellular Response on Electrospun Nanofibers for Tissue Engineering. *J. Biomater. Appl.* **2009**, *24*, 7−29.

(9) Mitik-Dineva, N.; Wang, J.; Truong, V.; Stoddart, P. R.; Malherbe, F.; Crawford, R. J.; Ivanova, E. P. *Escherichia coli*, *Pseudomonas aeruginosa*, and *Staphylococcus aureus* Attachment Patterns on Glass Surfaces with Nanoscale Roughness. *Curr. Microbiol.* **2009**, *58*, 268−273.

(10) Mitik-Dineva, N.; Stoddart, P. R.; Crawford, R. J.; Ivanova, E. P. Adhesion of Bacteria *Wiley Encyclopedia of Biomedical Engineering*; Wiley, Hoboken, NJ, 2006; Vol. *6*, pp 1−11.

(11) Kargar, M.; Ji, W.; Amrinder, N. S.; Bahareh, B. Controlling Bacterial Adhesion to Surfaces Using Topographical Cues: A Study of the Interaction of *Pseudomonas aeruginosa* with Nanofiber-Textured Surfaces. *Soft Matter.* **2012**, *40*, 10254−10259.

(12) Venugopal, J.; Ramakrishna, S. Applications of Polymer Nanofibers in Biomedicine and Biotechnology. *Appl. Biochem. Biotechnol.* **2005**, *125*, 147−157.

(13) Hsu, L. C.; Fang, J.; Borca-Tasciuc, D. A.; Worobo, R. W.; Moraru, C. I. Effect of Micro- and Nanoscale Topography on the Adhesion of Bacterial Cells to Solid Surfaces. *Appl. Environ. Microbiol.* **2013**, *79*, 2703−2712.

(14) Shellenberger, K.; Logan, B. E. Effect of Molecular Scale Roughness of Glass Beads on Colloidal and Bacterial Deposition. *Environ. Sci. Technol.* **2001**, *36*, 184−189.

(15) Advincula, M. C.; Petersen, D.; Rahemtulla, F.; Advincula, R.; Lemons, J. E. Surface Analysis and Biocorrosion Properties of Nanostructured Surface Sol-Gel Coatings on Ti6Al4V Titanium Alloy Implants. *J. Biomed. Mater. Res.* **2007**, *80B*, 107−120.

(16) Siddiqui, A. R.; Bernstein, J. M. Chronic Wound Infection: Facts and Controversies. *Clin. Dermatol.* **2010**, *28*, 519−526.

DOI: 10.1021/acsami.5b00453
ACS Appl. Mater. Interfaces 2015, 7, 7644−7652